Title

CHEMISTRY AND MORPHOLOGY OF COAL LIQUEFACTION ANNUAL REPORT, OCT. 1, 1981 - SEPT. 30, 1982.

Author

Heinemann, H.

Publication Date

1982-10-01

LBL-15095
UC-90 c.2

Lawrence Berkeley Laboratory
UNIVERSITY OF CALIFORNIA

Materials & Molecular Research Division

CHEMISTRY AND MORPHOLOGY OF COAL LIQUEFACTION
ANNUAL REPORT
October 1, 1981 - September 30, 1982

Heinz Heinemann

October 1982

Prepared for the U.S. Department of Energy under Contract DE-AC03-76SF00098

DISCLAIMER

ANNUAL REPORT

October 1, 1981 - September 30, 1982

CHEMISTRY AND MORPHOLOGY OF COAL LIQUEFACTION

Contract ET-78G-01-3425

Principal Investigator: Heinz Heinemann

Lawrence Berkeley Laboratory

University of California

Berkeley, California 94720

This work was jointly supported by the Director, Office of Energy Research, Office of Basic Energy Sciences, Chemical Sciences Division and the Assistant Secretary for Fossil Energy, Office of Coal Research, Liquefaction Division of the U. S. Department of Energy under Contract DE-AC03-76SF00098 through the Pittsburgh Energy Technology Center, Pittsburgh, PA.

This manuscript was printed from originals provided by the author.

CONTENTS

I TECHNICAL PROGRAM FOR FISCAL 1982

Task 1 - Selective Synthesis of Gasoline Range Components from Synthesis Gas - A. T. Bell

Analytical methods will be developed to better define product distribution in each carbon number product (n/i ratio, paraffin/olefin ratio) and to test the Schultz-Flory theorem for each hydrocarbon type. This will also permit distinction between primary and secondary products. The extent of olefin saturation and hydrogenolysis will be investigated. Tests will be conducted with iron catalysts prepared on either ZSM-5 type zeolites or carbon molecular sieves. The emphasis of this work will be on determining the effect of the support structure and composition on the distribution of products obtained. The degree to which the formation of high molecular weight products can be curtailed by this means will be examined as a function of support pore size and composition, as well as reaction conditions.

Task 2 - Electron Microscope Studies of Coal During Hydrogenation - J. W. Evans

The major research activity in 1982 will be the use of the environmental cell in the Hitachi 650kV transmission electron microscope to observe reactions between carbonaceous materials (with and without catalysts present) and gases. Plans are to start with oriented graphite then later use coal char and finally coal. Gaseous atmospheres would be water vapour, hydrogen or mixtures of the two. Reaction products will be identified by analysis of the gas leaving the cell using the mass spectrometer. This will also permit a semi-quantitative measurement of reaction rate by simultaneously measuring the flow rate of gaseous reactant into the cell.

Some additional investigations of coal microstructure may be carried out as time permits.

Task 3 - Catalysed Low Temperature Hydrogenation of Coal - G. A. Somorjai

Exploration of the mechanism of alkali catalyzed reactions of carbon and steam will include attempts to detect CH_x and COH intermediates by electron spectroscopy and exploration of the possibility of alkali intercalation into the graphite that may be an important reaction step needed to break the C-C bonds of the reactant efficiently. The use of alkaline earth compounds as possible catalysts will be investigated to optimize the activity of the carbon-water ($C-H_2O$) reaction. The combination of transition metals and alkali-metal compounds as catalysts should be explored in order to aid the formation of hydrocarbon molecules larger than CH_4.

Task 4 - Selective Hydrogenation, Hydrogenolysis and Alkylation of Coal and Coal Liquids by Organo-Metallic Systems - K. P. C. Vollhardt

The Lewis acid catalyzed cleavage and alkylation of benzene will be investigated in great detail. Scope and limitations will be explored with a variety of substrates, particularly substituted benzenes and higher condensed aromatic molecules. Heteroaromatic systems will be exposed to similar reaction conditions. The mechanism of the reaction will also be subjected to scrutiny, using kinetic and labeling techniques.

An investigation of the potential use of transition metals as catalysts and/or reagents in the cleavage of aromatic carbon-carbon bonds with the particular aim to effect hydrogenation and hydrogenolysis will be begun.

Work will continue concerned with delineating mechanism and scope of transition metal mediated hydrogen shifts of organic π ligands.

Task 5 - Chemistry of Coal Solubilization and Liquefaction
T. Vermeullen, and R. H. Fish

Plans for FY 1982 are to move into the area of metal-catalyzed transfer hydrogenation. We intend to begin by investigating metal complexes which serve either as hydrogenation or dehydrogenation catalysts, and determine whether they will function as transfer hydrogenation agents. If we are successful in finding workable systems, we will then investigate their mechanisms with an eye toward understanding the transfer hydrogenation in general, and improving the efficiency of the catalysts which are uncovered.

Further work will be done on the important selective hydrogenation of N-containing rings in polynuclear aromatic hydrocarbons with homogeneous catalysts, discovered in 1981. In particular, the question of catalyst recovery, e.g., by heterogenizing the metallo-organic complex will be investigated.

Task 6 - Coal Conversion Catalysts - Deactivation Studies -
A. V. Levy and E. E. Petersen

Short term plans are a series of experiments similar to those already carried out, but at much more stringent conditions; i.e., higher metal concentrations, higher temperatures, and longer times. The objective of these studies is to deactivate the catalyst sufficiently to observe changes in the global rates of demetallation and desulfurization. The deactivated catalysts will be subjected to electron microprobe measurements, and transient diffusion measurements as well as more traditional surface area, porosimetry, and pore volume measurements to evaluate the chemical and physical factors contributing to deactivation.

All of the results to date have been obtained using vanadyl napthenate. We envision a series of runs using vanadyl tetraphenylporphyrin to compare with the naphthenate results. We also envision a similar series using analogous titanium compounds. Although these metalloporphyrins are more representative of the metal constituents of residua and coal derived liquids, their solubility in hydrocarbon solvents is limited. Steady-state experiments rather than semibatch will be used. Also, to make the desulfurization global activity measurements easier, we plan to add dibenzothiophene as the sulfur component.

II HIGHLIGHTS

Task 1:

1) A gas chromatic system was developed which permits complete on-line analysis of all products from Fischer-Tropsch synthesis.

2) Dependence of synthesis rates on H_2 and CO partial pressures and temperatures have been determined. The data suggest that formation of light hydrocarbons can be reduced at low H_2/CO ratios and at high total pressures.

3) At low conversion the primary C_2 hydrocarbons are α-olefins and the primary oxygenates are C_2 aldehydes. With increasing conversion the olefin/paraffin ratio decreases and aldehydes are converted to alcohols.

Task 2:

1) Using an environmental cell within the 650 keV transmission electron microscope, the potassium hydroxide catalyzed gasification of graphite has been observed. Thereby it has been shown that controlled atmosphere electron microscopy is a powerful tool for identifying suitable catalysts for carbon reactions and determining their mode of action.

2) Work on this project has substantially contributed to Task 3.

Task 3:

1) A steady state production of methane and CO_2 in

equimolar amounts is obtained from high density graphite and water at 225-375°C in the presence of KOH or K_2CO_3 on the graphite surface.

2) Indications are that higher hydrocarbons can be produced.

3) When the reaction of graphite with water is carried out in the presence of calcium oxide, no methane is obtained, but graphite carbon is converted to an active carbon which can be hydrogenated to methane.

4) Graphite samples intercalated with potassium produce methane when reacted with water, but at a much slower rate than when KOH is present on the external surface.

5) Reaction of graphite and water occurs on the edges of graphite planes.

Task 4:

1) A detailed analysis of the volatile hydrocarbons obtained from the reaction of benzene and $AlCl_3$ has been performed. Several experiments point to the intermediacy of phenylcyclohexane as a primary product. ^{13}C-^{12}C exchange is observed using a 1:1 mixture of $^{13}C_6H_6$ and $^{12}C_6H_6$. Predominant hydrogenation is noted when polybenzenoids are reacted with $AlCl_3$ in the presence of PtO_2/H_2. Cycloalkanes, however, undergo mainly ring contraction reactions. Significant suppression of polymer formation occurs in the cracking of saturated and benzenoid hydrocarbons in the $AlCl_3Pt/H_2$ system.

2) Novel thermal and light mediated C-C and C-H bond breaking and bond forming processes have been uncovered in the coordination sphere of cobalt. These involve diene ligands of the type thought to be potential intermediates in aromatic hydrocarbon hydrogenation and hydrogenolysis. Detailed mechanistic investigations have been undertaken.

Task 5:

The following has been demonstrated:

1) Selective hydrogenation of nitrogen heterocyclic rings in model coal compounds using transition metal carbonyl hydrides as catalysts in homogeneous reactions.

2) Selective hydrogenation of model coal compounds using Wilkinson's catalyst $[(\phi_3P)_3RhCl)]$ in both the homogeneous and heterogenized forms.

3) Catalytic transfer hydrogenation reactions utilizing saturated nitrogen heterocyclic compounds as the hydrogen source and transition metal complexes as the hydrogen shuttle agent. For example, using 9,10-dihydrophenanthridine and $(\phi_3P)_3Cl$, hydrogen was transferred to quinoline giving phenanthridine and 1,2,3,4-tetahydroquinoline.

4) Control experiments verify $(\phi_3P)_3RhCl$ as the dehydrogenating agent in the reactions with 9,10-dihydrophenanthridine. Additionally, oxygen increased the rate of dehydrogenation of 9,10-dihydrophenanthridine, but only in the presence of $(\phi_3P)_3RhCl$.

5) Deuterium gas experiments (D_2) with phenanthridine gave evidence for reversibility in the hydrogenation reaction as well as hydrogen exchange for deuterium on the aromatic ring. The latter exchange reaction must occur via a cyclometallation reaction. Similar results with quinoline further defined the cyclometallation, but exchange experiments with undeuterated tetrahydroquinoline establishes a different mechanism for deuterium incorporation at the position alpha to nitrogen in tetrahydroquinoline.

6) In initial competitive experiments to define the relative reactivities of the coal model compounds, it was found that thiophene did not inhibit the hydrogenation of quinoline with $(\phi_3P)_3RhCl$ as catalyst.

7) Pyridine, a mononuclear nitrogen heterocyclic compound inhibits the hydrogenation of quinoline. This result implicates basicity as a criteria for reduction, i.e., the more basic nitrogen heterocyclic compound, pyridine, inhibits quinoline reduction by competitive coordination to rhodium.

Task 6:

1) A model has been developed to simulate the deactivation of a catalyst pellet during desulfurization and demetallation.

2) Metallic deposits on the surface of the catalyst change the reactivity of the catalyst not only by diffusion restriction into the smaller pores, but also by acting as catalysts themselves.

3) The main feature of the model is that it permits calculation of the parameters from the pore size distribution of the catalyst as the pore sizes change during the catalyst life.

III SUMMARY OF STUDIES

Task 1: Selective Synthesis of Gasoline Range Components from Synthesis Gas - A. T. Bell, Task Manager

The research carried out during the past year has been aimed at three principal objectives. The first was to develop a capability for complete online analysis of the products produced during Fischer-Tropsch synthesis. The second objective was to determine the influence of reaction conditions on the synthesis of hydrocarbons and oxygenated products over an iron catalyst contained in a well-stirred slurry. The third objective was to establish whether olefins, produced as a primary product of Fischer-Tropsch synthesis undergo significant further chain growth and whether the recycle of olefins can be used to obtain non-Schulz-Flory product distributions.

Proper analysis of reaction products is essential to understanding the effects of catalyst composition and reaction conditions on the kinetics of Fischer-Tropsch synthesis. For the purposes of the present task, a gas chromatographic system was developed which permits a complete on-line analysis of all products to be performed in about an hour. A 1/8 in. by 9 ft. stainless steel column packed with Chromsorb 106 is used to separate CO, CO_2, C_1 through C_5 hydrocarbons, as well as acetaldehyde and acetone; C_4 through C_{30} hydrocarbons and oxygenates are separated on a 50 m glass capillary column coated with OV 101. The identity of the major, and many of the minor products have been established by GC/MS.

The synthesis of hydrocarbons over a fused Fe catalyst, promoted with potassium, has been studied in a well-stirred autoclave. The product distribution changes with time and

approaches a Schulz-Flory distribution asymptotically. Each product approaches the steady-state distribution with a time constant which depends on the molecular weight and Henry's Law constant of the product in the paraffin wax used to suspend the catalyst. A mathematical model of the evolution of the product distribution was found to describe the observed results very successfully and to explain many anomalies in the published literature.

The dependence of the synthesis rates on H_2 and CO partial pressures, and temperature have been determined. It is observed that the H_2 dependence is unity for all products. The CO dependence is -0.42 for methane and increases to zero for C_4. This suggests that the formation of light hydrocarbons can be reduced at low H_2/CO ratios and high total pressures. The activation energies for all products were nearly the same, lying between 26 and 29 kcal/mole. At low conversions the primary C_{2+} hydrocarbons are α - olefins and the primary oxygenates are C_{2+} aldehydes. As conversion increases, the olefin to paraffin ratio decreases slightly and the aldehydes are converted increasingly to alcohols. Very little methanol is produced at any conversion level.

Experiments were conducted to test whether the feedback of olefins could be used to alter the product distribution. For these runs, a fixed bed reactor was operated at 305°C and 5 atm, using a H_2O/CO of 2 in the feed gas. To simulate olefin feedback, 5% of ethylene, propylene, or cis-2-butene was added to the sythesis gas feed. It should be noted that the concentration of added olefin is much greater than that present due to synthesis alone. The addition of ethylene causes a 60% increase in the production of propylene and no more than a 10% increase in the production of butenes. The balance of the

products are unaffected by ethylene addition. The addition of propylene causes a 15% increase in the formation of butenes and a slight increase in the formation of ethylene, but has no other effect. The only effects of cis-2-butene addition are a 40% increase in propylene formation and a slight increase in ethylene formation. In each of the cases examined, the proportion of the added olefin converted to products of greater chain length is only a few percent. From these results, it is concluded that small olefins do not enter into the chain growth process very efficiently, and in fact may undergo hydrogenolysis to produce lower molecular weight products.

Reference: "An Explanation for Deviation of Fischer-Tropsch Products From a Schulz-Flory Distribution" by A. T. Bell, and R. A. Dictor, I&EC Process Design and Dev., Submitted.

Task 2: Electron Miscrosope Studies

J. W. Evans, Task Manager

Controlled atmosphere electron microscopy (CAEM) has been used to examine high density pyrolytic graphite during the course of reaction with water vapor in argon, catalyzed by potassium and sodium hydroxide. Thin specimens of highly oriented pyrolytic graphite were mounted on electron micrope grids and dipped into 0.38M potassium hydroxide solution. After drying the specimens were mounted on a heating stage and placed into a Gatan "environmental cell" within a Hitachi 650 keV transmission electron microscope. Argon, at approximately 1 atmosphere pressure was bubbled through water at room temperature, giving an Ar/H_2O ratio of about 40/1, and then introduced into the environmetal cell to give a pressure of 50 Torr. The specimens were heated in the flowing gas mixture and periodically observed. At 500°C the potassium hydroxide was dispersed as particles 0.1 - 0.5μm in diameter on the surface of the graphite. With increasing exposure time, gasification was evident as the particles at the edges of the graphite crystals began moving toward the crystal centers leaving channels in their wake.

Figure 1 shows two micrographs recorded 11 minutes apart taken from a sequence showing the channel growth at 500°C. Channels are evident in two adjacent graphite crystals emanating from the edges of the crystals, each channel with a particle at its head. The interface between the particles in the channels and the graphite shows a hexagonal, faceted morphology. As the reaction continues the particles move and the length of the channels increase, as can be seen by the particles arrowed. The channels remain roughly parallel sided indicating that there is little effect of uncatalyzed reaction at the channel edges, or of wetting of the channel sides by catalytic material. Initially particles lying on the surface of the graphite crystals do not

contribute to the catalytic gasification of the carbon. At a later stage, however, faceted pits in the graphite are evident at the former positions of these particles. The catalyst particles are present within, and at one edge of, the pits. In some cases chanelling by these particles away from the original pits is evident.

Similar observations have been noted at 600°C. At this temperature, however, no "incubation" period was noted for the catalytic reaction involving the particles dispersed on the surfaces of the graphite crystals and widespread channelling due to gasification was observed from outset. Figure 2 shows two micrographs taken from the same area undergoing catalytic gasification at 600°C under the same gas conditions as before. The micrographs were taken 10 minutes apart and the first was taken after only 2 minutes exposure. Some of the catalytic particles are large and form wide channels up to $\sim 1 \mu m$ wide, extending from the edge of the crystal. Chanelling is also evident originating at pits, away from the edges of the crystal, again with particles at the heads of the channels. The channels are not straight-sided and there is a general enlarging of the pits. This suggests a wider dispersion of the catalytic phase, possibly as a liquid, forming a thin film along the crystal edges and around the edges of the pits.

These studies show that potassium hydroxide is effective in catalyzing the steam gasification of graphite and that the mode of the catalyzed attack is a channelling one with each channel being headed by a particle of sodium compound. Similar observations of the catalysis by sodium and calcium compounds have been made in the Berkeley microscope.

Reference: "An Electron Microscopy Study of the Low Temperature Catalysed Steam Gasification of Graphite" by D. J. Coates, J. W. Evans, A. L. Cabrera, G. A. Somorjai, and Heinz Heinemann, J. Catalysis, in Press.

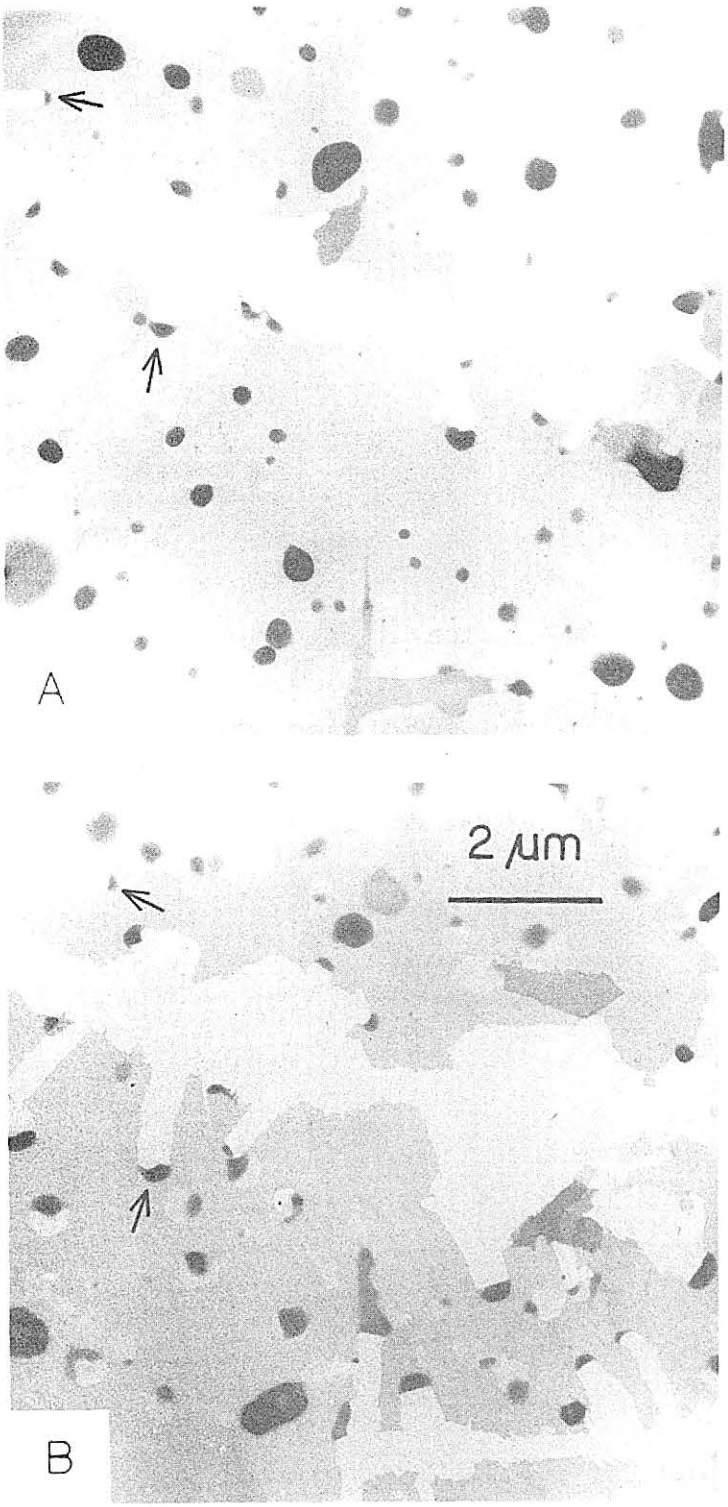

Figure 1 XBB 824-3397

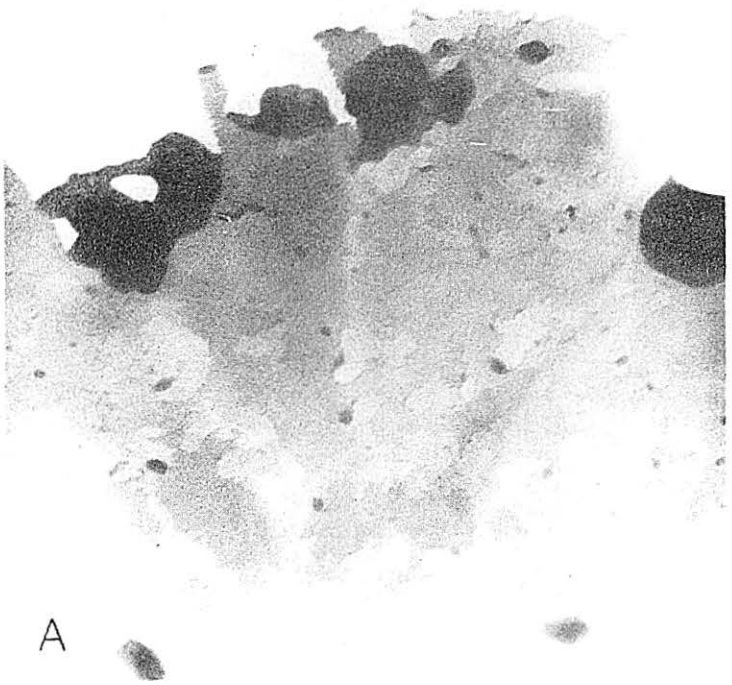

A

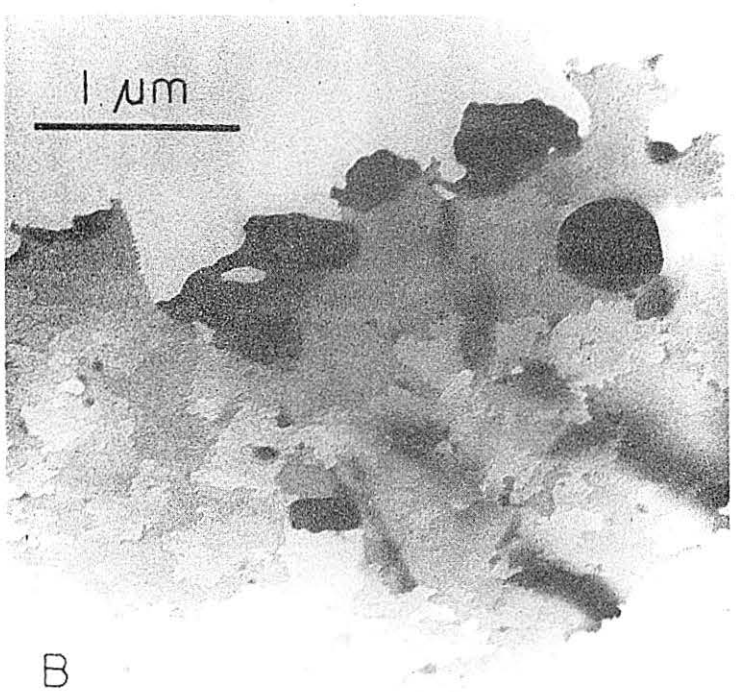

B

Figure 2

XBB 824-3396

Task 3: Catalyzed Low Temperature Hydrogenation of Coal
G. A. Somorjai, Task Manager

The Purpose of these studies is to produce high molecular weight hydrocarbons by the catalyzed depolymerization and hydrogenation of carbonaceous solids (graphite, char, etc.).

A) Methane Production From the Alkali Hydroxide Catalyzed Reaction of Graphite with Water Vapor at Low Temperatures (500-600K)

The steady state production of methane from the catalyzed reaction of high density graphite and water vapor at low temperatures (500-600K) is reported. The reaction is catalyzed by potassium hydroxide and potassium carbonate placed on the graphite surface. The steady state production of methane has a turnover frequency of 10^{-3} sec^{1} at 522K and an activation energy of 10 ± 3 kcal/mole. Several other alkali hydroxides, e.g., lithium, sodium, and cesium hydroxide all turned out to be good catalysts for the production of methane from water vapor and graphite. The surface composition and surface texture were characterized by Auger electron spectroscopy and scanning electron microscopy, respectively.

The production of gaseous CH_4 and CO_2 (or CH_4 and CO) from graphite occurs rapidly in the temperature range 500-650K with low activation energy (10 ± 3 kcal) in the presence of alkali compounds. KOH, K_2CO_3, LiOH, CsOH, and NaOH all appear to catalyze both the reduction of C to CH_4 and its oxidation to CO_2 or CO.

Using high surface area graphite, we have shown that scaling up the C/H_2O reaction to produce large amounts of CH_4 gas can readily be accomplished. Thus this reaction can be carried out under technologically feasible conditions. One should then consider other, more economical, sources of carbon to

produce CH_4, such as coal, biomass, including wood, or other plant sources. Initial experiments show that production of C_2 and higher hydrocarbons is feasible.

B) Calcium Oxide Catalyzed Low Temperature Methane Production From Graphite

Calcium oxide catalyzes the transformation of graphitic carbon to an active form of carbon in the presence of water vapor:

$$(\text{graphite}) \xrightarrow{CaO, H_2O} C_{(\text{active})}.$$

This transformation could be monitored by x-ray photoelectron spectroscopy and its activation energy is 16.3 kcal/mole. Methane formation only occurs in the presence of hydrogen as the active carbon is gasified with an activation energy of 25.5 kcal/mole:

$$C_{(\text{active})} + 2H_2 \xrightarrow{CaO} CH_4.$$

C) Study of Potassium Intercelated Graphite

Potassium intercelated graphites C_8K and $C_{24}K$ have been employed for our reaction studies using water vapor. The rate of methane production is much lower for the intercelated samples than when KOH was on the external surface of the pure graphite sample. It appears that alkali catalyst intercelation plays no important role during gasification.

D) Electron Microscopy and Reaction Rate Studies of the Structure Sensitivity of Graphite Gasification

Electron microscopy studies in the transmission mode using an environmental cell revealed that the reaction preferentially occurs at the edges of the graphite planes. As gasification proceeds channels are cut into the graphite sample

and the KOH catalyst is located at the end of the channel where gasification takes place at the catalyst-graphite interface.

These results were also confirmed by reaction rate studies using different surface area and thickness graphite samples. While increasing the basal plane area of graphite did not increase the reaction rate, increasing the thickness (edge area) increased the methane production rate in proportion.

References: A. L. Cabrera, Heinz Heinemann, and G. A. Somorjai, "Methane Production from the Catalysed Reaction of Graphite and Water Vapor at Low Temperatures." J. Catalysis, 75, 7, 1982.

Task 4: Selective Hydrogenation, Hydrogenolysis, and Alkylation of Coal and Coal Related Liquids by Organometallic Systems - K. P. C. Vollhardt, Task Manager

A) Finalizing Studies on the Reaction of Benzene with Aluminum Chloride

The reaction of benzene with aluminum trichloride has been studied under many different conditions, and generally a complex mixture of hydrocarbons is obtained. However, the nature of the major products reported varied greatly in the early experiments, and the accuracy of the structure assignments might be held in doubt due to insufficient separation and characterization of the product mixtures. A detailed analysis of the volatile components of the reaction has never been performed.

Heating benzene and $AlCl_3$ in a glass pressure vessel under various conditions furnished alkybenzenes in addition to a variety of other products (Table 1). Application of pressure, however, reduced the number of products (resulting in cleaner GC traces) and their overall yield.

A typical GC trace of the reaction of benzene with $AlCl_3$ is shown in Figure 1, the four major products being toluene, ethylbenzene, tetralin and biphenyl (Table 1).

The reaction always yields some polymeric materials, believed to contain polyphenyls. The monitored reaction (Figure 2) also shows an initial build-up of polynuclear aromatic hydrocarbons such as methylphenanthrenes, methylanthracenes and phenylnaphthalenes which are known to undergo Scholl-type polycondensation reactions in the presence of $AlCl_3$.

TABLE 1. Product yields from the reaction of benzene and $AlCl_3$ under various reaction conditions.

CONDITIONS :	$[AlCl_3]$ = 0.25M 200°C, 3h $[W(CO)_6/diphos]$[b], H_2(100 atm)/ CO(20 atm)	$[AlCl_3]$ = 0.25M N_2(120 atm), 200°C, 3h	$[AlCl_3]$ = 0.7M N_2(1 atm), 160°C, 48h	$[AlCl_3]$ = 0.7M $[PtO_2]$ = 2.2×10^{-4}M H_2(6.8 atm)[c], 160°C, 7.5h[d]
% Yield[a] of :				
Toluene	1.07, (0.97)[e], (1.13)[f]	1.15	2.19	0.49
Ethylbenzene	1.66, (1.75)[e], (2.07)[f]	1.34	2.68	1.98
i-Propylbenzene	0.17, (0.04)[e], (0.14)[f]	0.05	0.18	0.03
n-Propylbenzene	trace, (0.07)[e], (0.01)[f]	0.09	0.33	0.21
Butylbenzene(s)	trace, (0.02)[e], (0.04)[f]	0.01	0.11	0.23
Tetralin	0.04, (0.04)[e], (0.05)[f]	0.02	0.73	1.20
Phenylcyclohexane	0.02, (0.01)[e], (0.03)[f]	0.01	0.06	1.50
Biphenyl	0.04, (0.13)[e], (0.16)[f]	0.08	1.55	0.37
Diphenylmethane(s)	5.97, (0.15)[e], (0.56)[f]	0.02	0.23	trace
Diphenylethane(s)	0.15, (0.06)[e], (0.28)[f]	0.02	0.34	0.21
Total % Yield	9.12, (3.24)[e], (4.47)[f]	2.79	8.40	6.22

[a] GC yield calculated using n-octane as internal standard. These products were characterized by GC/MS and coinjection of authentic samples.

[b] $[W(CO)_6]$ = [diphos] = 4.7×10^{-3}M.

[c] Periodically repressurized when hydrogen was consumed.

[d] Most benzene was reduced to cyclohexane after 6-7 hours under these conditions.

[e] Yield from reaction in the absence of $W(CO)_6$.

[f] Yield from reaction in the absence of diphos.

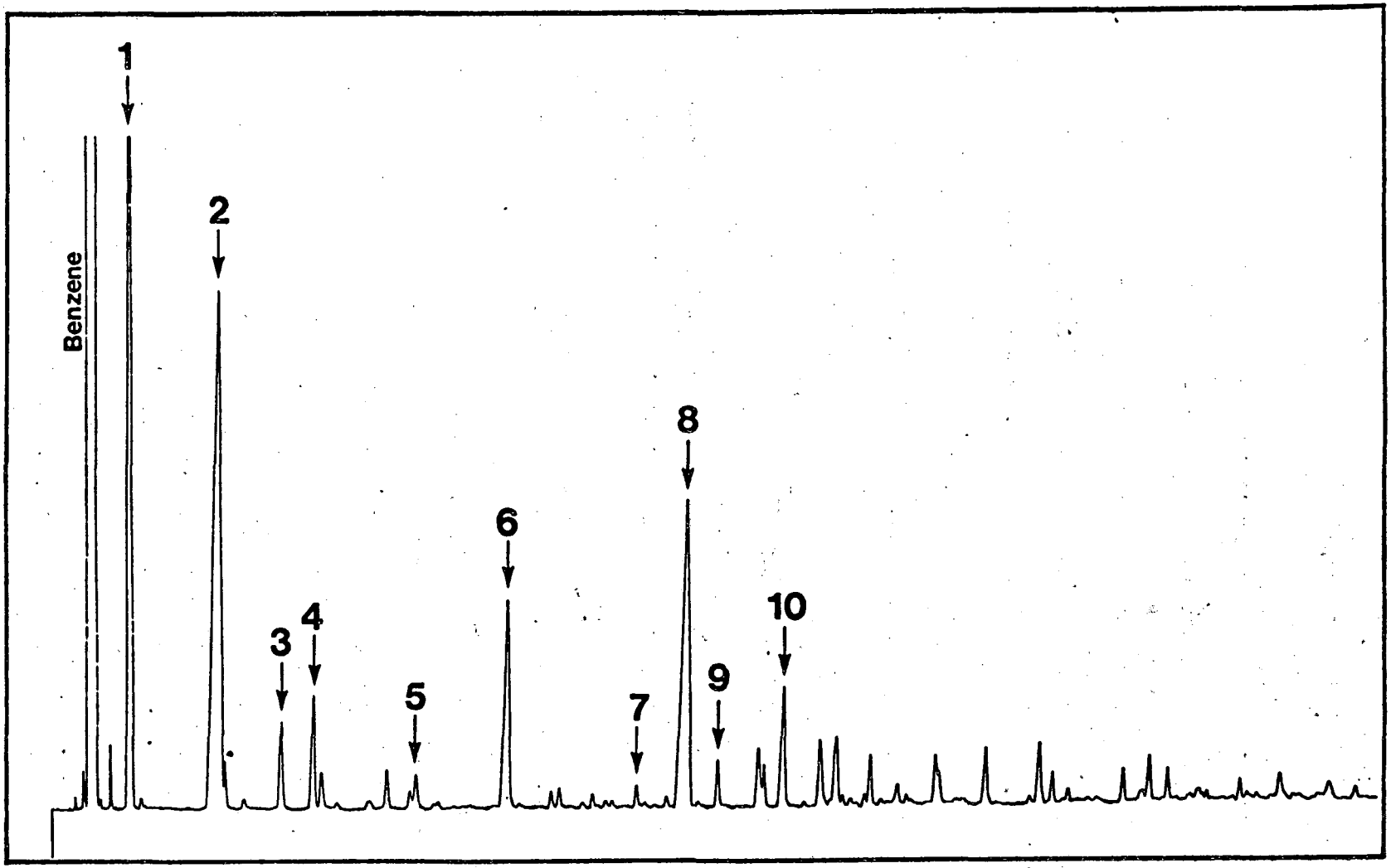

Fig. 1. A typical GC trace of the products from the reaction of benzene and $AlCl_3$ ($[AlCl_3]$ = 0.7M, N_2(1 atm), 160°C, 48h). 1 = toluene, 2 = ethylbenzene, 3 = isopropylbenzene, 4 = n-propylbenzene, 5 = butylbenzenes, 6 = tetralin, 7 = phenylcyclohexane, 8 = biphenyl, 9 = diphenylmethane, 10 = 1,2-diphenylethane. 1-10 were identified by GC/MS and coinjection of authentic samples. Other minor products were (GC/MS computer library): methyl-, dimethyl-, and ethyltetralins, phenylcyclopentane, fluroene, methyl- and ethylbiphenyl, 1,1-diphenylethane, phenylnaphthalene, and phenyltetralin.

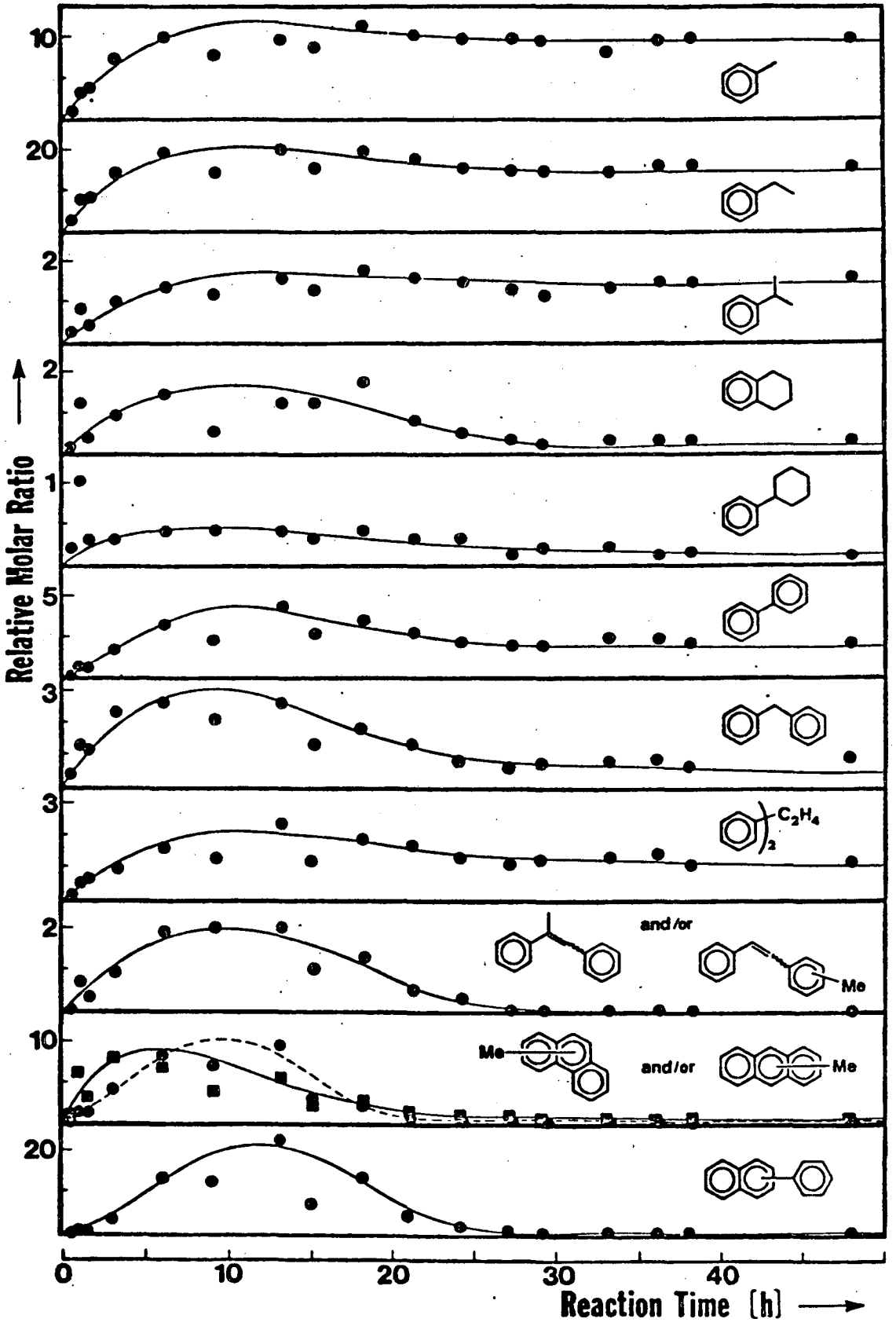

Fig. 2. Plot of relative molar ratio of selected products vs. reaction time in the $AlCl_3$/benzene reaction ([$AlCl_3$] = 0.7M, N_2(1 atm), 160°C, 48h). n-Octane was used as internal standard. Different scales have been used for clarity. Smooth curves are drawn arbitrarily.

In order to minimize polymerization and condensation reactions, several experiments were carried out under hydrogen in the presence of a catalytic amount of PtO_2. Hydrogen consumption was fairly rapid and as expected the reaction was much cleaner. The product mixture essentially contained the same alkylbenzenes as found in the reaction of benzene with $AlCl_3$ alone with, however, a markedly increased amount of phenylcyclohexane which now replaced biphenyl as one of the four major products (Table 1; Figure 3). Schemes 1-4 depict plausible pathways enroute to products.

Several labeling experiments were performed. Reaction of C_6D_6 gave completely labeled products. Not unexpectedly, a 1:1 mixture of C_6H_6 and D_6D_6 gave complete scrambling. Therefore an equimolar mixture of C_6H_6 and $^{13}C_6H_6$ (90% enriched) was exposed to $AlCl_3$ [N_2(1 atm), 160°C, 48h]. Surprisingly, ^{13}C-^{12}C exchange (ca.5%) was observed in recovered "unreacted" benzene and additional scrambling in all other volatile products as analyzed by GC/MS. The mass spectral peak patterns indicate substantially intact incorporation of alkyl chains derived from the original benzene ring. Thus, the connectivity of the initial carbon arrays is extensively preserved in the alkybenzenes (including annulated and cycloalkylbenzenes) formed. The mechanism by which label exchange occurs is not understood at present.

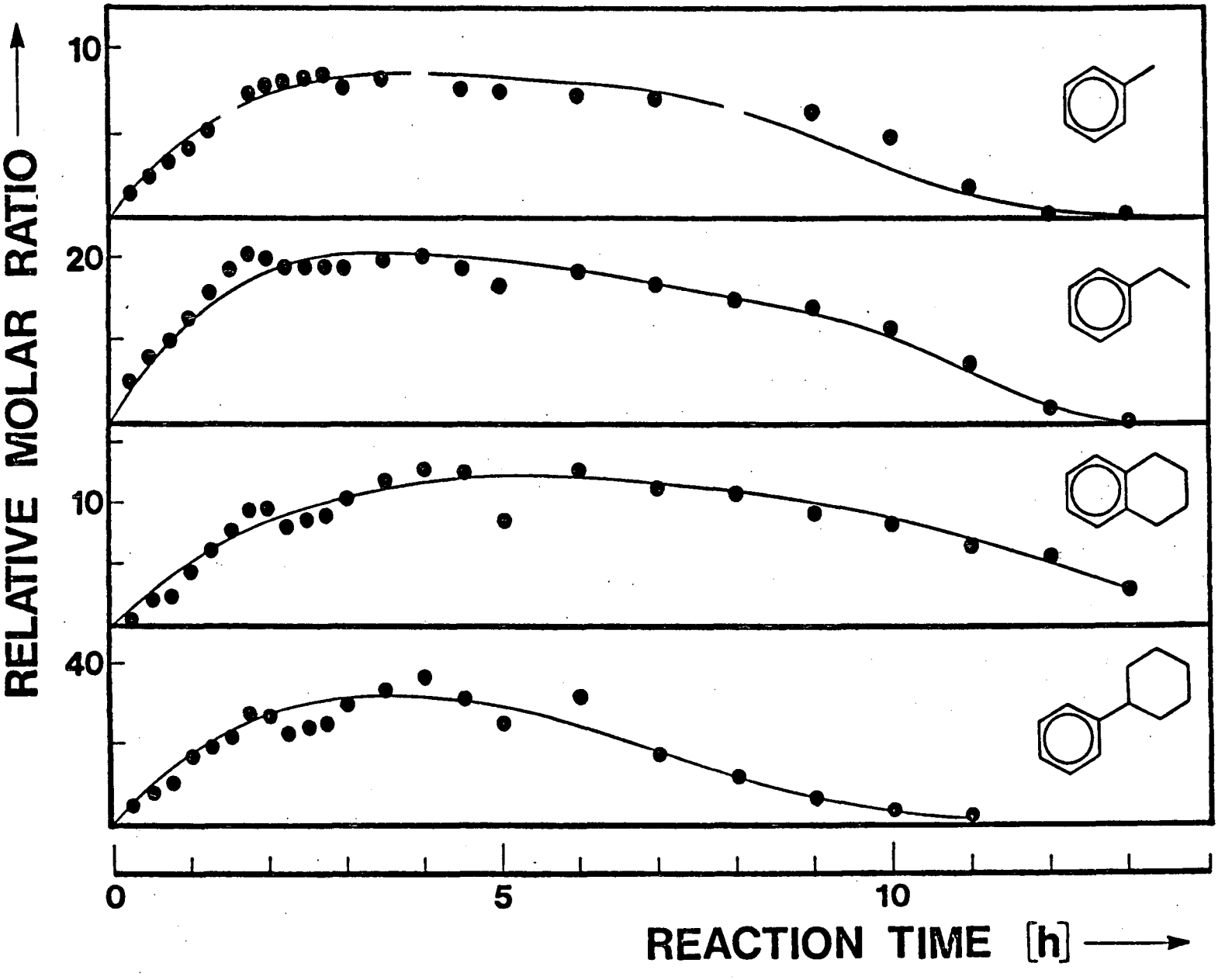

Fig. 3. Plot of relative molar ratio of toluene, ehtylbenzene, tetralin and phenylcyclohexane vs. reaction time in the $AlCl_3$/benzene/H_2/PtO_2 reaction ([$AlCl_3$] = 0.7M, H_2 (6.8 atm), 160°C, 13h). n-Octane was used as internal standard. Difference scales have been used for clarity. Smooth curves are drawn arbitrarily

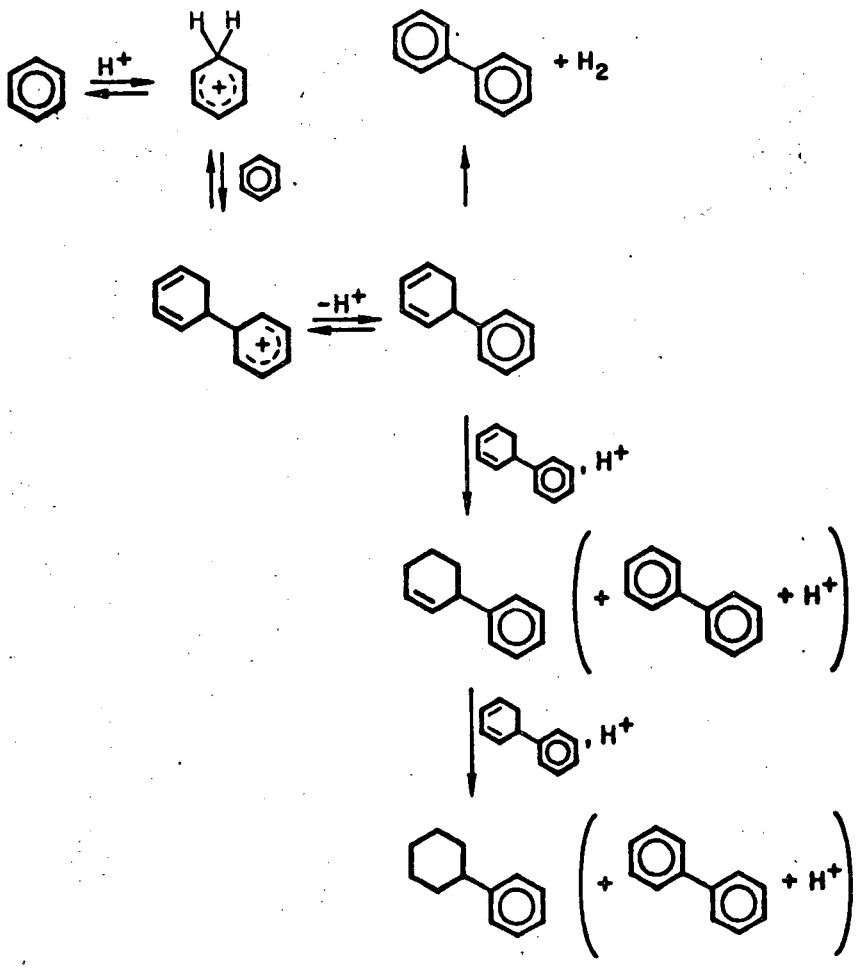

SCHEME 1 Formation of phenylcyclohexane and biphenyl via disproportionation of phenylcyclohexadiene.

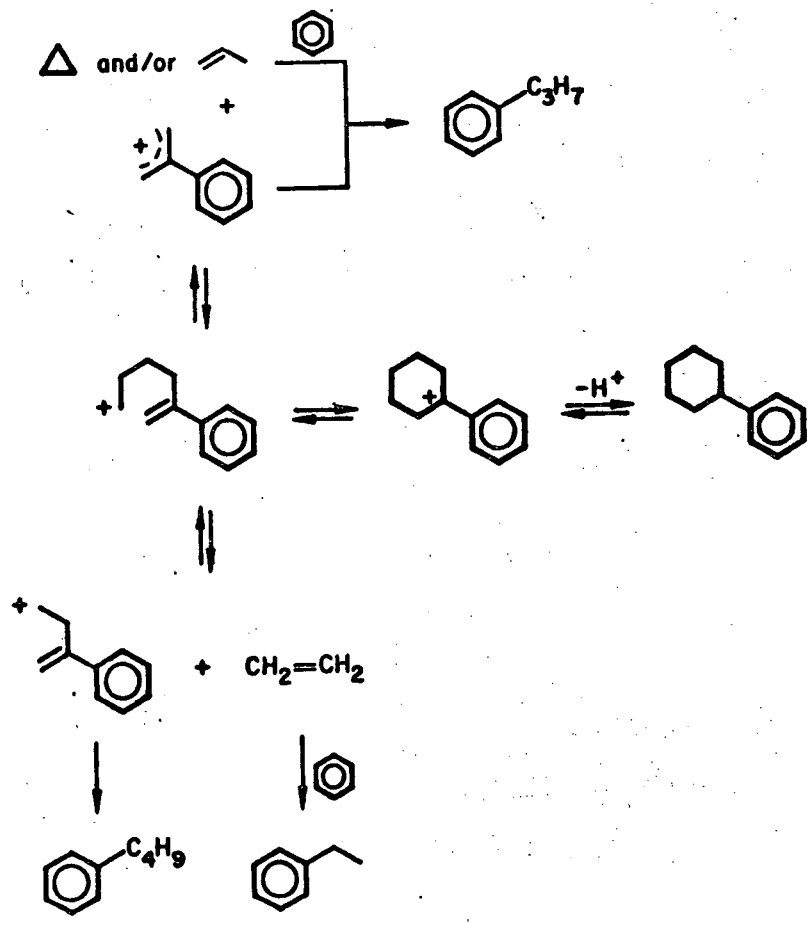

SCHEME 2 Proposed selected fragmentation reactions of phenylcyclohexane to furnish alkylbenzenes.

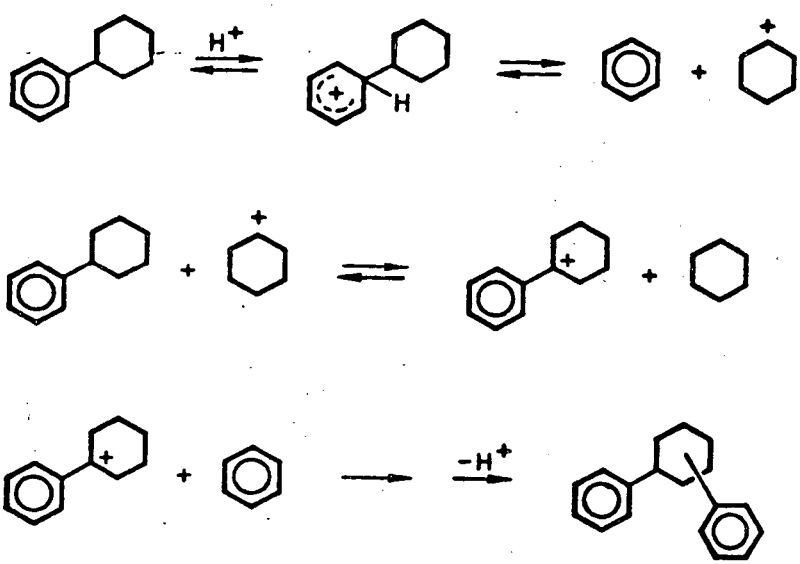

SCHEME 3 Formation of diphenylcyclohexane(s) from dealkylation-transalkylation of phenylcyclohexane.

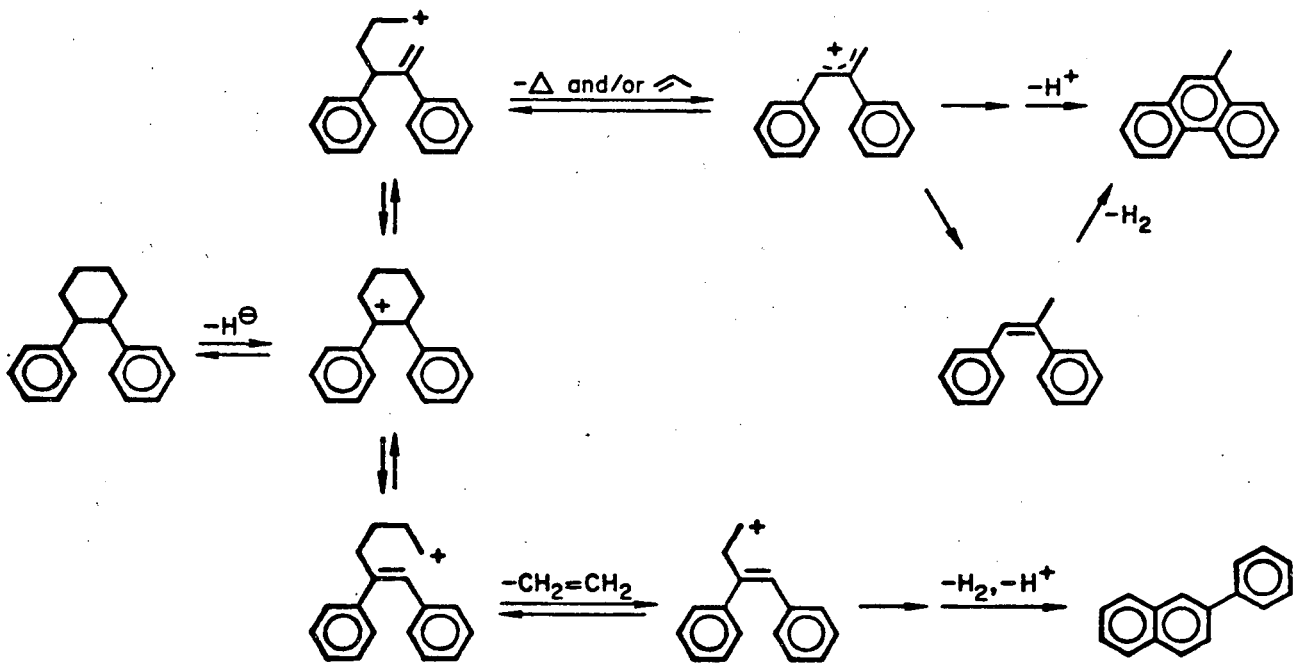

SCHEME 4 Proposed fragmentation reactions of diphenylcyclohexane(s) to furnish some of the observed polybenzenoids.

An extension of our investigation involved the $AlCl_3$-induced cracking of some cycloalkanes and polynuclear aromatic hydrocarbons under hydrogenation conditions as models for the hydroliquefaction of coal and/or heavy petroleum hydrocarbons. The results are summarized in the Schemes below. In these reactions there was insubstantial polymer formation, in contrast to the other studies. The reaction of larger cycloalkanes gives mainly ring contraction products.

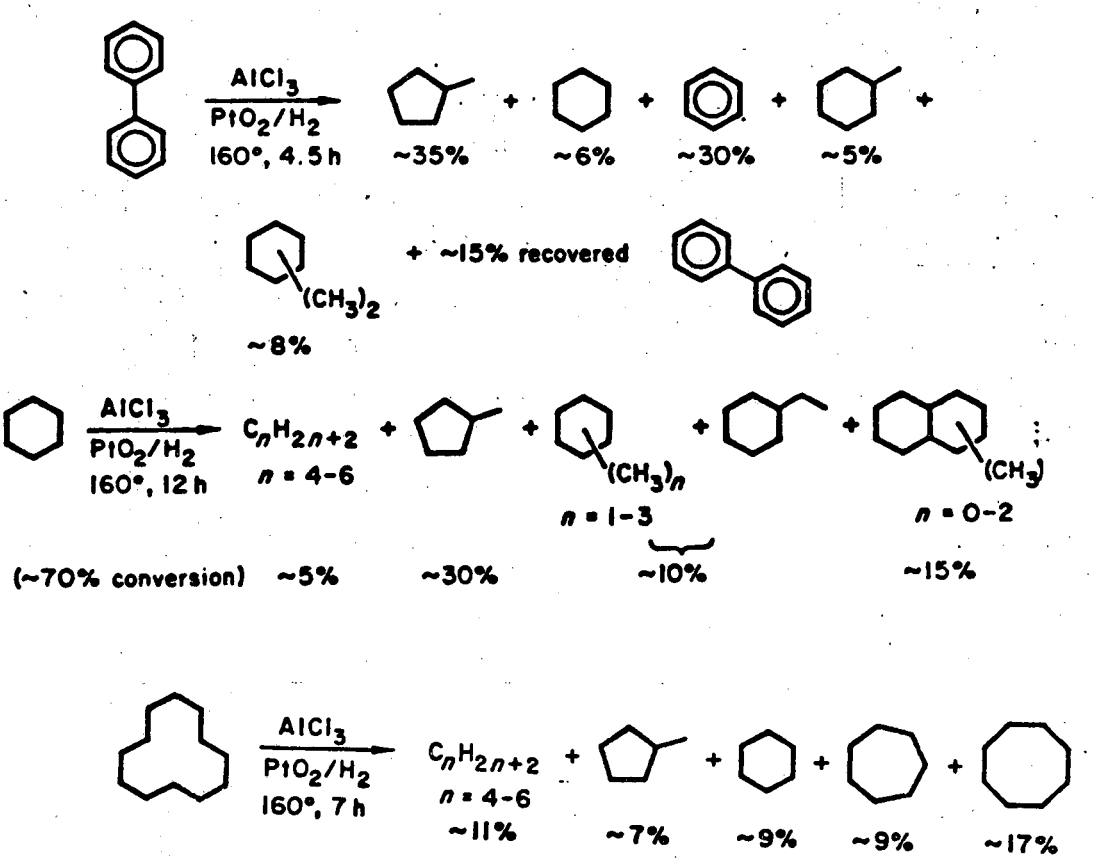

It is clear that many of the reactions described in this paper will play a significant role in any process that attempts to liquefy coal or heavy petroleum hydrocarbons in the presence of Lewis acids. It appears that the use of Lewis acid alone leads to polymerization and subsequent catalyst deactivation. On the other hand, simultaneous application of a platinum hydrogenation catalyst and hydrogen, although successfully minimizing polymerization, results in secondary reactions, such as premature hydrogenation competing favorably with the cracking of hydrocarbons. A successful method for hydroliquefaction of coal would seem to depend on the search for a bifunctional catalyst having complementary properties of Lewis acid and hydrogenation activity.

B) Diene Cobalt Complexes as Models for Hydrogenolysis of and Hydrogenshifts in Coal Unsaturates

We have postulated the theoretical feasibility of aromatic hydrocarbon hydrogenolysis by a route involving an initial arene → dihydroarene step followed by a metal promoted ringopening to a complexed oligoene:

Proposal:

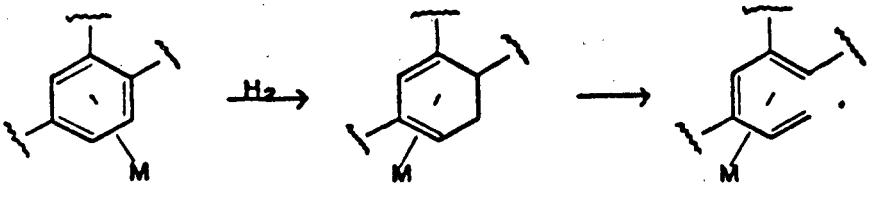

(1)

If successful, this could provide a long sought and unique method for coal hydrogenolysis. This proposal has prompted an investigation of the thermal and photolytic chemistry of transition metal diene and triene complexes, models for the last two species in (1).

We have found that CpCo-η^4-cyclohexa-1,3-diene (Cp=η^5-C_5H_5) is remarkably stable thermally with respect to ring opening, but that it undergoes relatively rapid intramolecular hydrogen shifts via intermediate metal hydrides (2). Moreover, on laser irradiation one can observe the desired ring opening

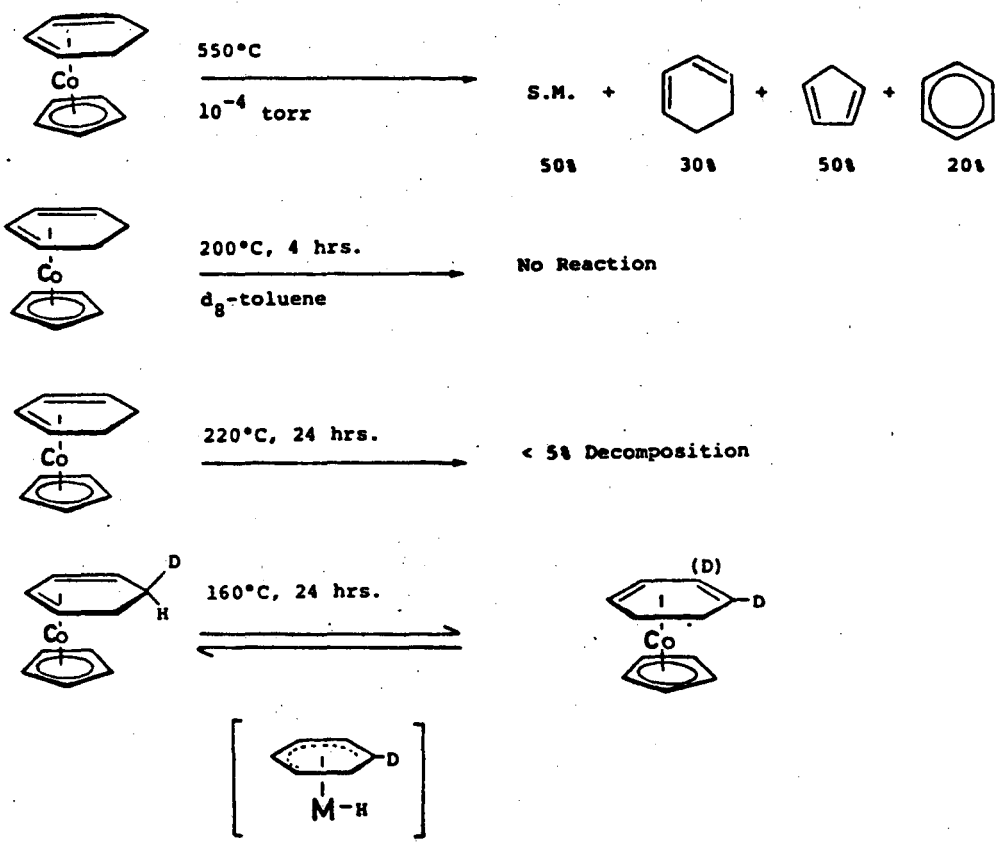

(2)

to CpCo-η^4-1,3,5-hexatriene, albeit with low quantum efficiency.

To probe the potentially adverse thermodynamics of the postulated ring opening it was planned to test the thermal behavior of CpCo-η^4-cis-1,3,5-hexatriene. For this purpose the complexation chemistry of the ligand under irradiative conditions was subjected to detailed scrutiny. A range of products

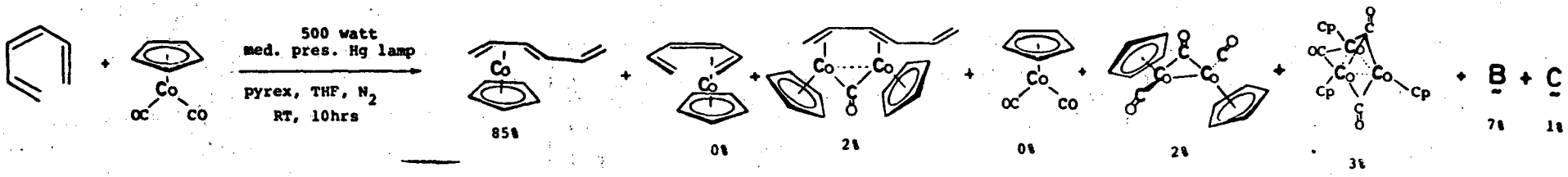
500 watt
med. pres. Hg lamp
pyrex, THF, N2
RT, 10hrs
85%
0%
2%
0%
2%
3%
7%
1%


413 nm, RT
1 hr
16%
27%
25%
26%
4%
2%
413 nm, RT
3 hrs
46 %
30 %
14%
6%
2%
2%
350 nm, RT
2.5 hrs
40 %
26 %
0%
29%
2%
2%
>404 nm
2 x 10-2 torr, -78°C
d8-Toluene, 3hrs
0%
0%
36%
62%
1%
1%

(3)

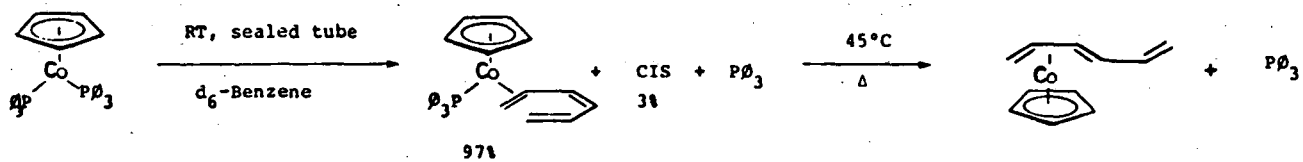
RT, sealed tube
d6-Benzene
97%
CIS + PØ3
3%
45°C
Δ
PØ3

(4)

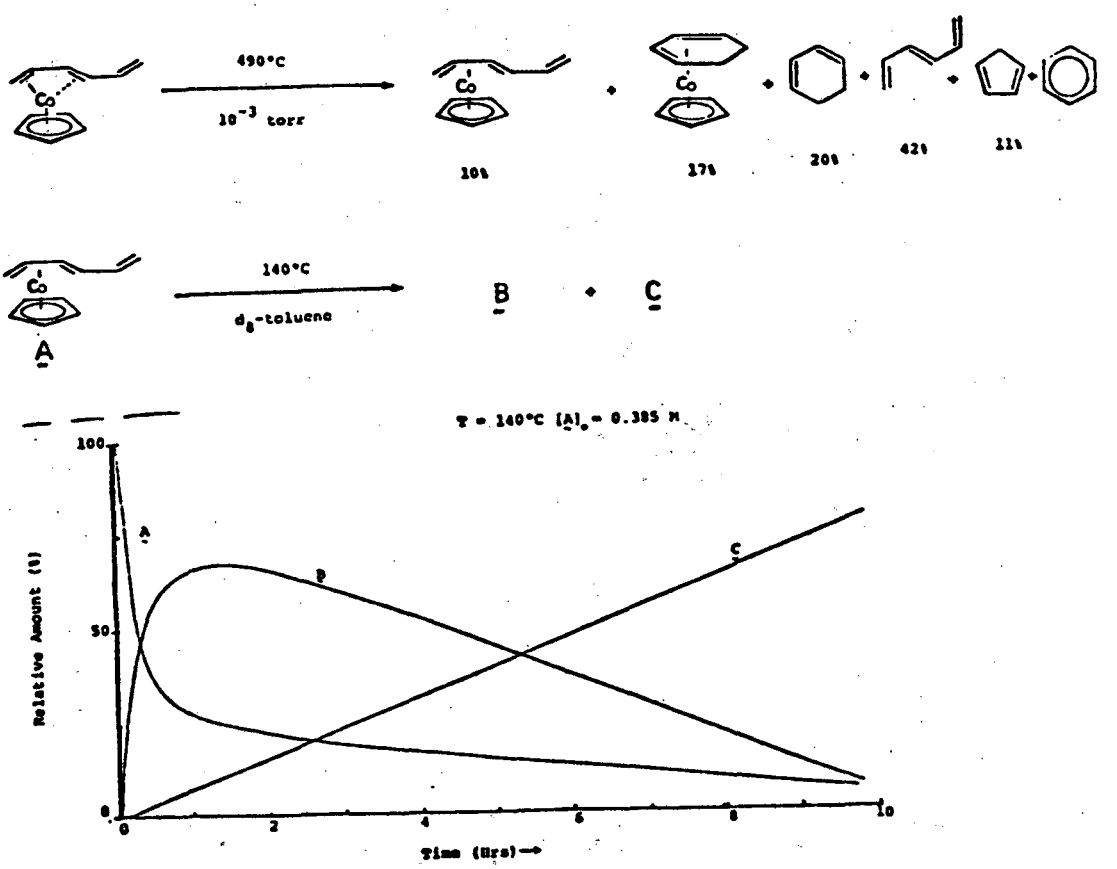

Scheme (5) Comparison of the gas phase and solution thermal chemistry of A. The lower graph depicts the relative amounts of A, B and C with time in the solution experiment.

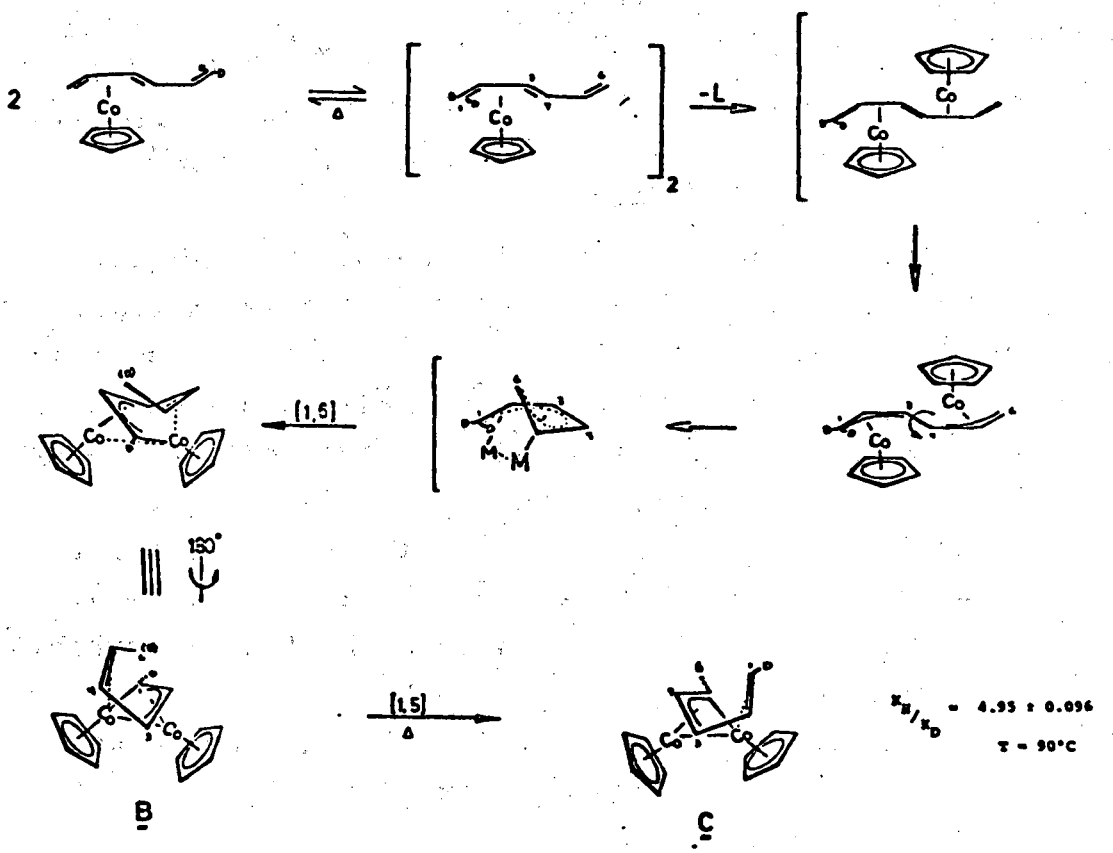

Scheme (6) Mechanism of the A→B→C sequence. The outcome of the deuterium labeling experiment is indicated by the appropriate lettering.

was observed (3), including some of the desired cis-complex, but also a substantial amount of the trans-isomer. The latter is the major compound on prolonged irradiation. We have established the mechanism of this isomerization through the investigation of labeled butadiene-CpCo. It proceeds through the intermediacy of a cobaltacyclopent-3-ene valence tautomer (equivalent to a ring flip) which exchanges inside substituents at the complexed diene termini with the outside ones. Scheme (3) also indicates ^{2}-diene complex formation [ascertained in (4)] and the emergence of small amounts of dinuclear complexes, in addition to two new compounds "B" and "C" (vide infra).

CpCo-trans-1,3,5-hexatriene A, Scheme (5) exhibits remarkable and unprecedented chemistry. In the gas phase mainly decomposition is observed, in addition to a small amount of the originally desired ring-closed 1,3-cyclohexadiene complex. In solution the dinuclear complexes B and C are formed, the X-ray structures of which were described in a previous report. Compound A first forms B which then undergoes a unimolecular rearrangement to C (Ea = 29.05 k cal mole^{-1}; Δ S = -8.37eu). The formation of B involves a 1,6 -hydrogen shift which exhibits a 100% strong deuterium isotope effect [Scheme (6)]. This has allowed us to pinpoint the regiospecificity of the subsequent hydrogen (deuterium) shift which connects B with C (Scheme 6).

This is supported by preliminary kinetic data on the A to B conversion (7). The initial [1,6] -shift occurs at temperatures as low as -20°C and thus might turn out to be one of the lowest activation energy vinyl-hydrogen activation processes known.

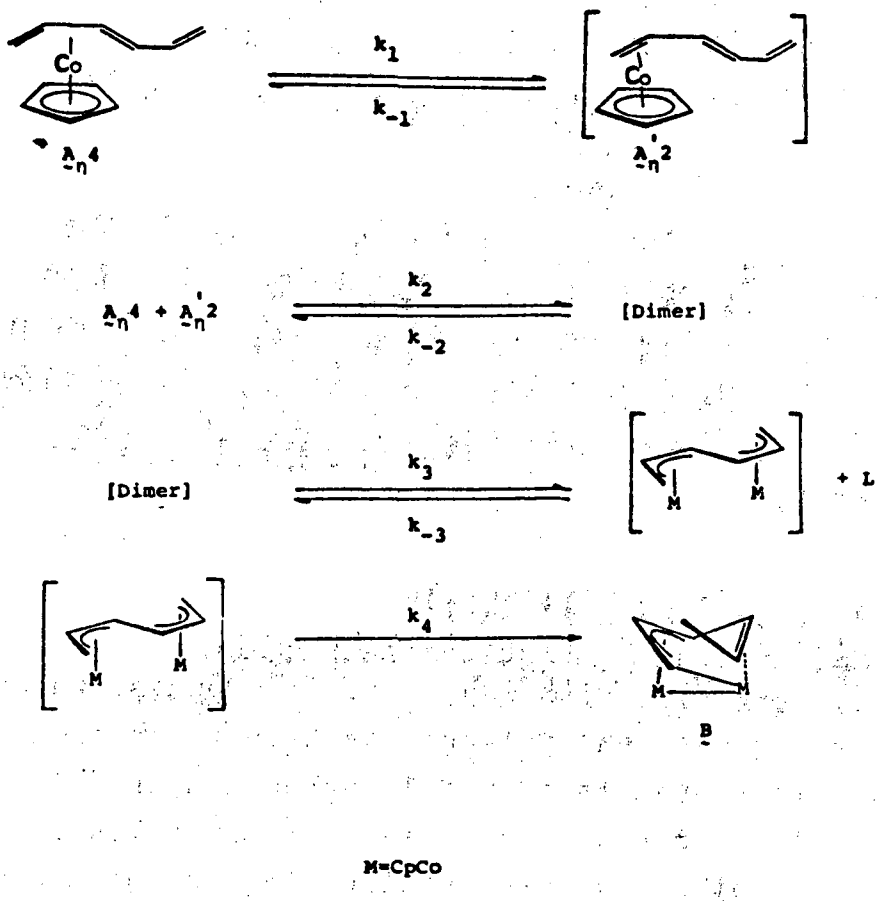

(7)

The reactions uncovered in this work constitute novel potential pathways by which hydrocarbons may transform on surfaces and in homogeneous catalytic hydrogenative and reforming systems. They also provide useful models for the possible chemistry of coal liquids when exposed to transition metal catalysts for the purposes of hydrogenation, desulfurization, and rearrangement.

Publications

1. Y.-H. Lai, L. S. Benner,, and K. P. C. Vollhardt, Studies on the Reaction of Benzene and Other Hydrocarbons with Aluminum Chloride. The Effect of Catalytically Activated Hydrogen, Fuel, in press.

2. Y.-H. lai, W. Tam, and K. P. C. Vollhardt, Transition Metal Activation of π-Complexed Benzene: Double Nucleophilic Addition, J. Organometal, Chem., 216, 97 (1981).

3. G. Ville, K. P. C. Vollhardt, and M. J. Winter, On the Reversibility of ^{4}-Cyclobutadiene Metal Formation From Complexed Alkynes: Unimolecular Isomerization of Labelled Racemic and Enantiomerically Enriched η^5-Cyclopentadienyl-η^4-cyclobutadiene Cobalt Complexes, J. Am. Chem. Soc., 103, 5267 (1981).

Task 5: Chemistry of Coal Solubilization

T. Vermeulen and R. H. Fish, Task Managers

We have demonstrated with model coal compounds, which include polynuclear aromatic and polynuclear heteroaromatic nitrogen compounds, that transition metal carbonyl hydrides, generated catalytically under a wide variety of conditions, selectively reduce the nitrogen heterocyclic ring in polynuclear heteroaromatic nitrogen compounds.[1] Moreover, we discovered that $(\phi_3P)_3RhCl$ or Wilkinson's catalyst will also selectively reduce the nitrogen containing ring in polynuclear nitrogen heterocyclic compounds under extremely mild conditions (80°, 300 psi H_2, for 2 hr.).[2]

With the latter catalyst $(\phi_3P)_3RhCl$), we also unvailed a dehydrogenation reaction with a saturated nitrogen heterocyclic compound, 9,10-dihydrophenanthridine, which provided the first example of a transfer hydrogenation using quinoline as the acceptor molecule.

The use of deuterium gas (D_2) in place of H_2 has given important insights into the hydrogenation reaction with phenanthridine and quinoline as substrates. The position alpha to the nitrogen in both dihydrophenanthridine (C_9) and quinoline (C_2) were deuterated. Additionally, exchange of an aromatic hydrogen for deuterium implicates cyclometallation reactions in both cases (Eq. 1 and 2).

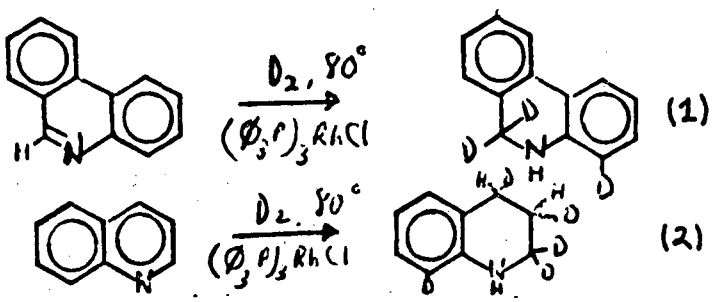

Initial competition experiments under hydrogenation conditions revealed several interesting facts: Quinoline in the presence of thiophene, with $(\phi_3P)_3RhCl$ as catalyst, provided tetrahydroquinoline with no apparent inhibition by thiophene. However, quinoline in the presence of pyridine was not hydrogenated implicating basicity as a criteria for reactions to occur. Possibly, pyridine acts, as CO did, to competitively inhibit by binding to rhodium and preventing quinoline from coordinating to the metal center.

References

1. R. H. Fish, A. D. Thormodsen, and G. A. Cremer, J. Am. Chem. Soc. 104, 0000, 1982.

2. R. H. Fish and A. D. Thormodsen, in preparation for Organometallics.

Task 6: Coal Conversion Catalysts-Deactivation Studies

A. V. Levy and E. E. Petersen, Task Managers

Catalysts used to hydrodesulfurize coal-derived liquids and petroleum residua are deactivated by the trace metals these liquids contain. The titanium in coal liquids and the vanadium in resids deposit on the external and internal surfaces of the catalyst thus both blocking access to the interior of the catalyst and covering active surface sites. Our objective is to examine this metal deposition process and how it affects desulfurization activity. We have approached the problem from three different angles: we have measured local metal deposition rates under realistic but experimentally manageable conditions; we have developed an extensive computer model describing the deactivation of a single catalyst pellet by metal deposits, and we have developed a technique to measure directly the decreased diffusivity of a catalyst containing metal deposits.

A comprehensive set of experiments using vanadium naphthenates as a model metal compound and a sour gas oil as a model liquid was completed during the past year. Stirred autoclave runs were made from 325°C to 400°C at vanadium levels of 100 to 400 ppm under 800 psig hydrogen and up to 48 hours in length. Catalysts samples were withdrawn periodically and analyzed for local metal concentration with a KEVEX X-ray microanalyzer across a polished cross-section. Radial concentration profiles of vanadium in catalysts samples taken at 8, 24, 32, and 48 hours are shown in Figure 1. The temperature was 325°C and the vanadium concentration 200 ppm as naphthenate. The amount deposited and the depth of penetration are much greater than in a similar run at 350°C presented last year, the general features are the same, however. Increased exposure time increases the amount of metal deposited and increases the deposit penetration. These profiles are indicative of a diffusion controlled reaction. A cross-plot of these data, showing the

change in vanadium concentration at a given depth versus time is presented in Figure 2. The slope of one of these curves is proportional to the rate of metal deposition at a given time for a given distance inside the pellet. The data fall in the order expected, the rate is slower deeper in the catalyst where concentrations of metal in the liquid are lower because of diffusion. The fact that deposition continues long after a monolayer of vanadium sufide is deposited demonstrates that vanadium sulfide is itself an active catalyst for demetallation. Note that the demetallation rates at all the interior points increase with time. This behavior can be explained by pore mouth poisoning of the demetallation reaction by vanadium sulfides. Because of diffusion limitations, vanadium deposits preferentially at the outside of the catalyst eventually building up a monolayer or more of sulfide and covering the active molybdenum-cobalt sulfide surface. This layer of vanadium sulfide is still active towards demetallation so deposition continues but at a slower rate than fresh catalyst. This slower rate gives vanadium in the liquid a greater chance to diffuse deeper into a catalyst pore so that the liquid concentration of vanadium increases over unpoisoned catalyst. The overall result is a shell of vanadium sulfide creeping towards the center of the pellet only partially inactivating it. Eventually enough metal may deposit at the exterior of the pellet to physically block all pores and stop the hydrodemetallation reaction completely.

Figure 3 shows smoothed radial concentration profiles of vanadium from catalysts run at four different temperatures and otherwise similar conditions. As expected for a diffusion-controlled reaction the apparent effectiveness factor decreases with increasing temperature, i.e., the profiles penetrate less deeply. However, the maximum demetallation rate at the outside edge where diffusion is not important decreases with increasing temperature instead of increasing as expected. The

most plausible explanation for this phenomenon is that homogeneous demetallation in the bulk liquid produces vanadium sulfide particles which reduces the concentration of vanadium naphthenate in the bulk solution and the net result is a decreased overall demetallation rate on the catalyst. Homogeneous demetallation is minimal at 325°C but is extensive at 400°C and is evidenced by the vanadium-rich sludge that settles out of diluted gas oil samples. The reduced effective concentration results in a lower reaction rate and smaller metal deposits at higher temperatures. Similar homogeneous demetallation of analogous iron compounds found during coal liquefaction could result in catalyst fouling and eventual bed plugging. Qualitatively then, the rate of demetallation on the catalyst and the depth of penetration within the catalyst decreases with increasing temperature because the effective concentration of reactants decreases and the Thiele parameter increases, respectively.

The experimental complications of the naphthenate-gas oil system, homogeneous demetallation, carbon deposition, and difficult sulfur analysis lead us to convert to a cleaner system consisting of white oil, metallo-porphyrins, and dibenzothiophene. Vanadyl porphyrins account for about 30 percent of the vanadium in residua. Coal-liquids are less well characterized but they do contain porphyrins and up to 70 percent of the titanium is reported to be organically bound although no direct evidence for titanyl porphyrins has been reported. A typical naphthenate and metallo-porphyrin are shown in Figure 4. We have chosen to sythesize metallo-porphyrins ourselves because vanadyl metallo-porphyrins contain impurities and titanyl porphyrins are not available. White oil contains no aromatics and therefore deposits coke much more slowly than gas oil. Dibenzothiophne is an excellent model of the more refractory sulfur compounds found in coal liquids. Having a

single sulfur compound, easily detectable by gas chromatography, alleviates the problems from the range of reactivities and the difficult combustion analysis associated with the spectrum of sufur compounds in gas oil. We have undertaken a set of experiments similar to the naphthenate runs with vanadyl tetraphenylporphyrin as well as some runs with titanyl tetraphenylporphyrin. Preliminary results indicate that titanyl and vanadyl porphyrins react similarly. Both demetallate at a higher rate than vanadyl naphthenate.

A model has been developed to simulate the deactivation of a catalyst pellet during the desulfurization and demetallation of a heavy oil. Unlike most catalytic reactions, a major product of the demetallation reaction remains behind on the catalyst surface. These deposits can directly change the reactivity of the catalyst and accumulation of the deposited material will restrict diffusion into the smaller pores of the catalyst, wherein much of the reactive surface is found. For most residua the metals are present, in a large proportion, in the asphaltene fraction in molecules whose dimensions are roughly equal to the diameters of the pores of the catalyst. There is a strong effect on the diffusivity if the ratio of reactant diameter to pore diameter is greater than 0.1. Therefore demetallation catalysts must have pore diameters which are large enough to pass the large metal-containing molecules and still provide the largest possible reactive surface area for economical use of the catalytic material and reactor bed volume. These catalysts must also be resistant to deactivation caused by the deposits which are built up during the lifetime of the catalyst. The objective of the modeling is to examine the resistance of different pore size distributions to deactivation so that catalyst improvements can be identified.

The model is based on the solution of the differential equations for diffusion and reaction in a catalyst pellet. The main feature of the model is the calculation of the model parameters from the pore size distribution of the catalyst as the pore sizes are altered during the lifetime of the catalyst.

References: Paper F in Session 1-b No. 8 of the AIChE meeting in Los Angeles, CA, November, 1982.

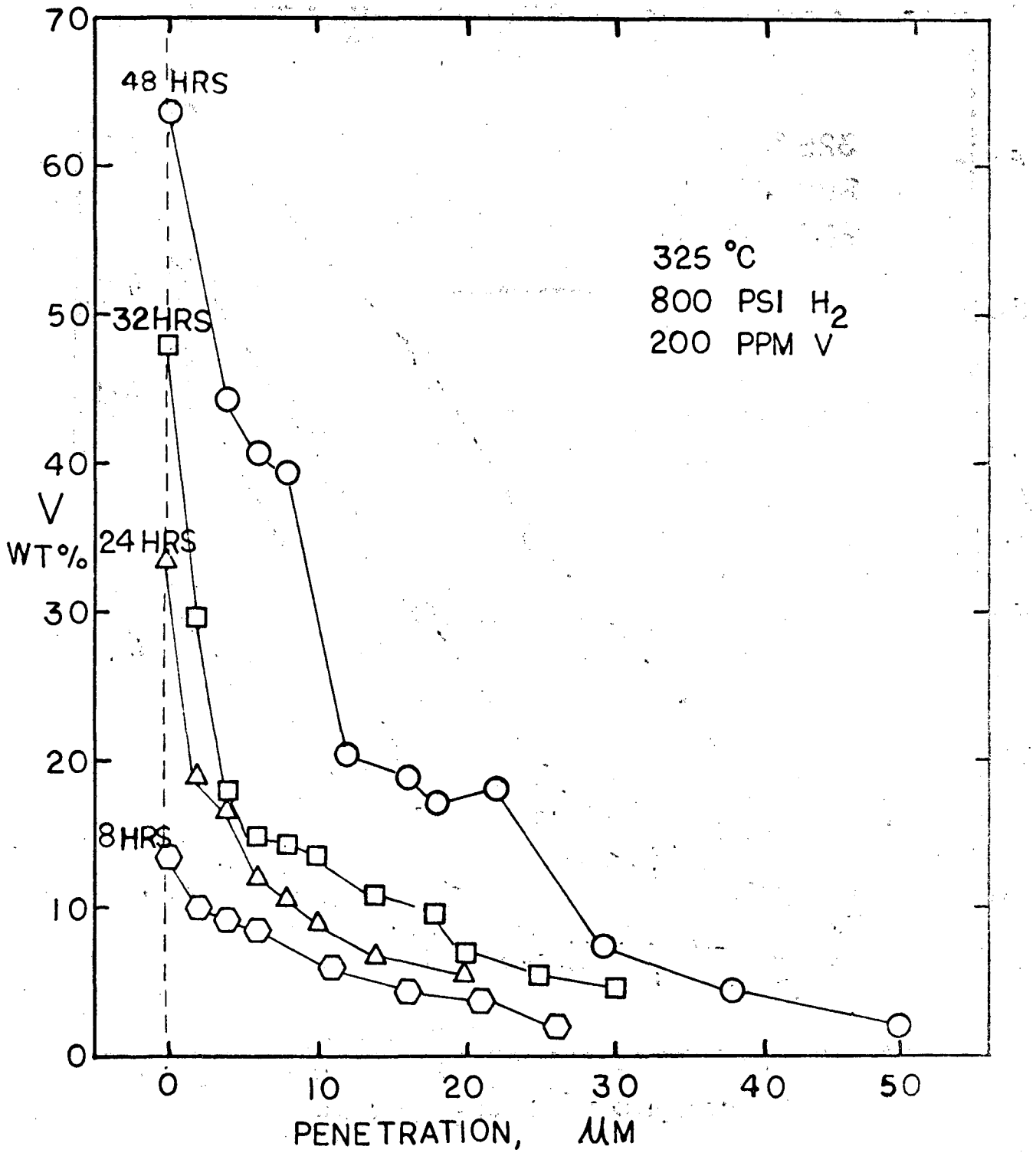
70
60
50
40
30
20
10
0
48 HRS
32HRS
24 HRS
8HRS
325 °C
800 PSI H_2
200 PPM V
V
WT%
0
10
20
30
40
50
PENETRATION, μM

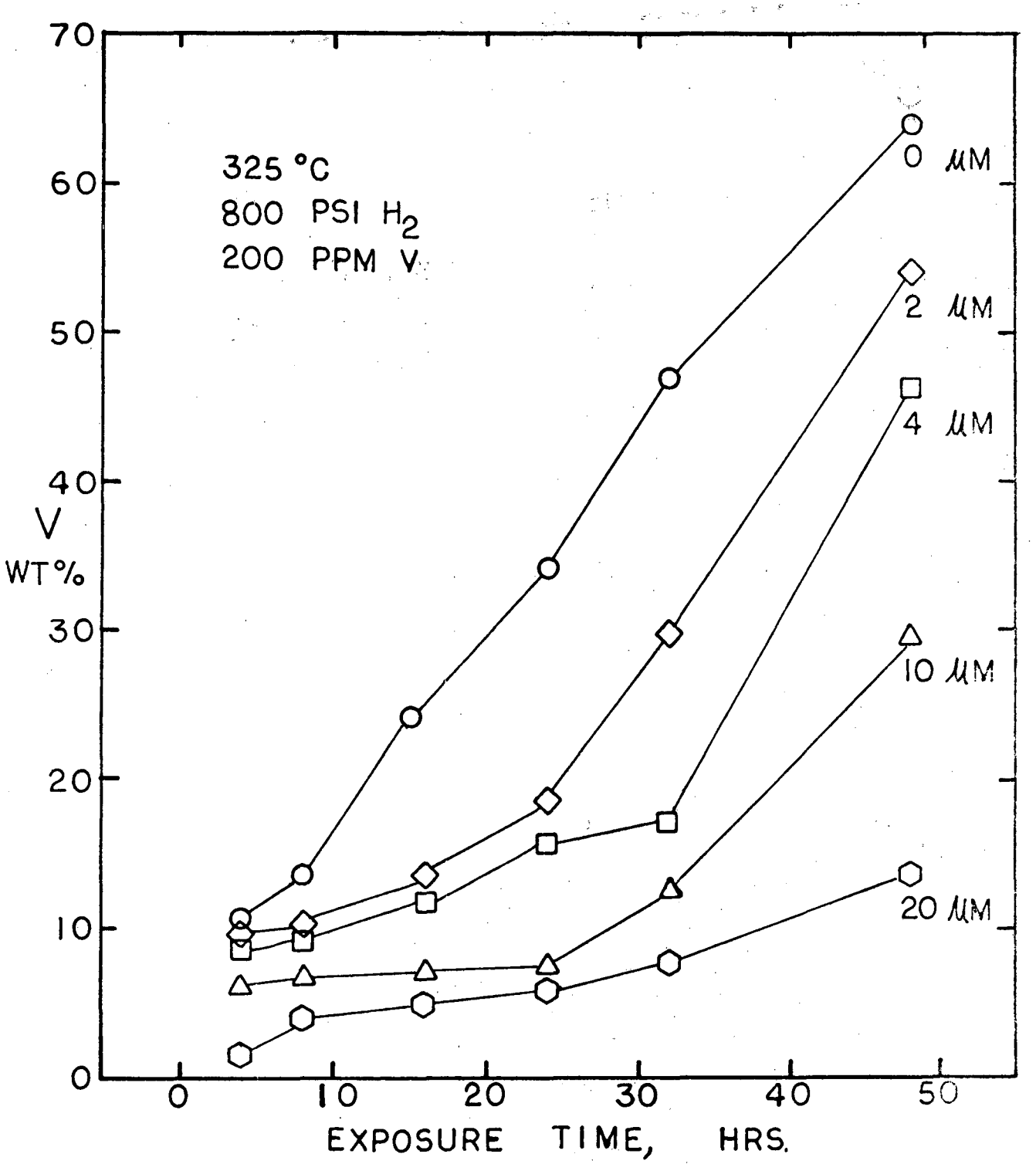
325 °C
800 PSI H_2
200 PPM V
0 μM
2 μM
4 μM
10 μM
20 μM
V
WT%
EXPOSURE TIME, HRS.
0
10
20
30
40
50
60
70

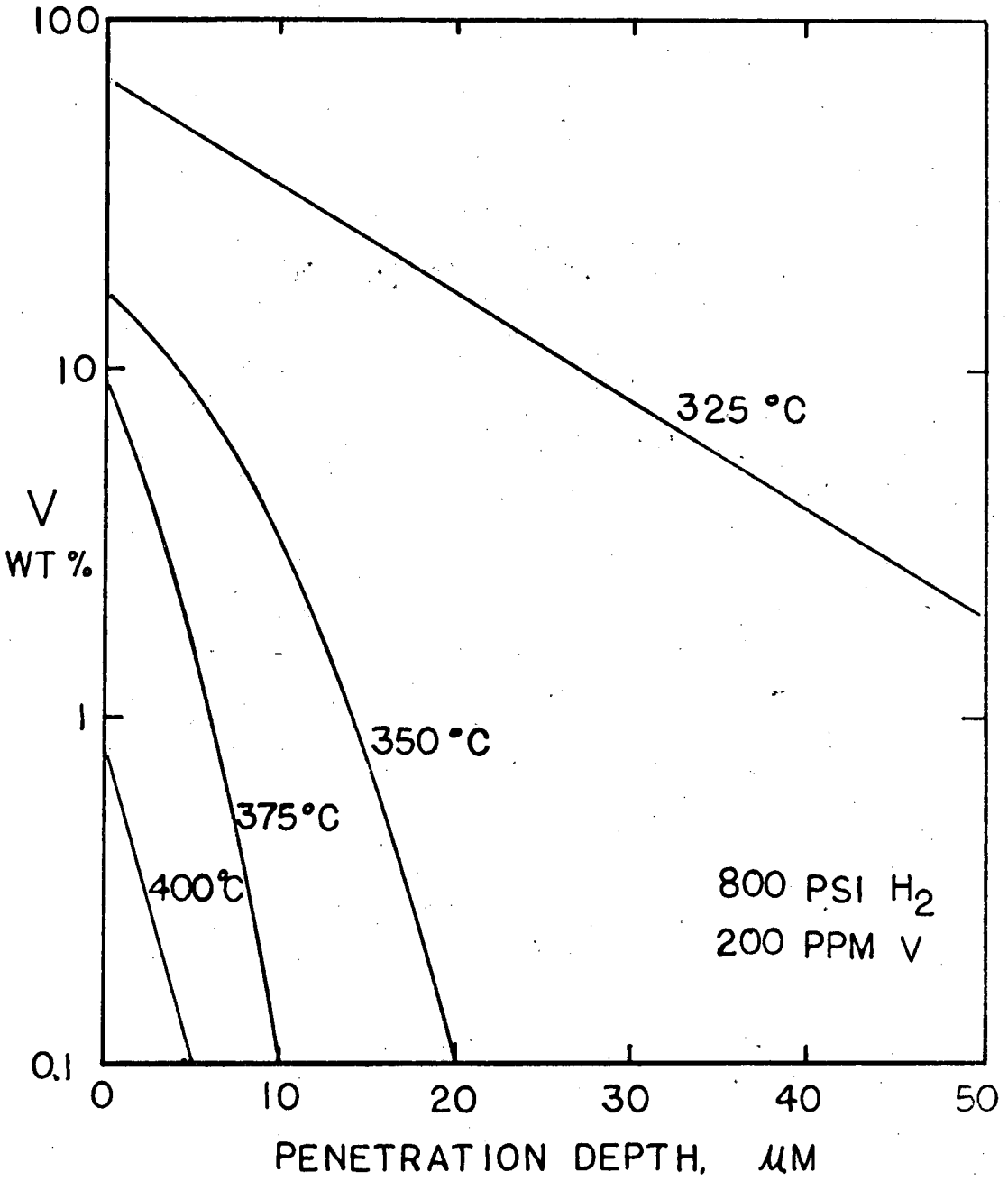
100
10
1
0.1
V
WT %
325 °C
350 °C
375°C
400°C
800 PSI H_2
200 PPM V
0
10
20
30
40
50
PENETRATION DEPTH, μM

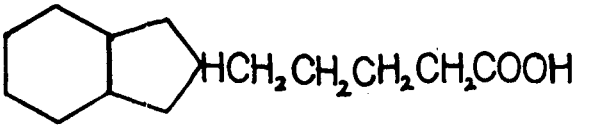

TYPICAL
NAPHTHENIC ACID

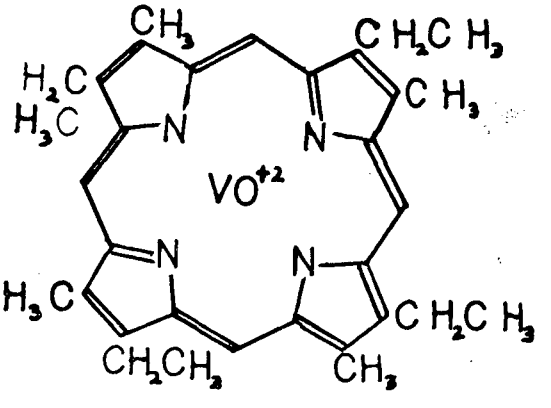

VANADYL ETIOPORPHYRIN

IV FUTURE RESEARCH PLANS

Task 1: Two major activities are planned for FY 1983. The first will be to complete the acquisition of rate data for Fischer-Tropsch synthesis over fused iron. The experimental effort will center on taking data at conditions simulating moderate to high CO conversion levels. The accumulated data will then be used to develop accurate rate and selectivity expressions. It will be of particular interest to establish whether a single rate expression can be used to describe the synthesis kinetics for a given product, over a wide range of syngas conversions.

Our second activity will be to determine the effects of support composition and pure structure on the distribution of synthesis products formed over supported iron catalysts. These efforts will be carried out with iron catalysts prepared on ZSM-5 type zeolites, carbon molecular sieves, and a variety of other supports, such as TiO_2, MgO, ZrO_2 and La_2O_3. Particular attention will be paid to the extent to which support characteristics influence the probability of chain growth, the formation of olefins versus paraffins, and the formation of oxygenated products.

Task 2: The catalysis studies described in this report will be continued in collaboration with Task 3 which is involved in "bulk" studies of carbon gasification catalysis. The work will be extended to coal chars and to minerals that are already present in coal (e.g. pyrite) and that may result in inherent catalysis during gasification.

Task 3: Major objectives during FY 1983 will be: Advancement of the mechanistic understanding of the catalysed graphite-water reaction; exploration of the promising area of

higher hydrocarbon production; methods to increase rates of hydrocarbon production; investigation of the behavior of char and coal.

Task 4: The thermal and photochemistry of aromatic and hydroaromatic ligands, as well as complexed oligoenes will be further explored. Work has begun using zirconium as a complexing agent, with its own unique chemistry. It is hoped that the special bonding capabilities of this metal will allow six-membered ring opening to be observable. Since it also has potential catalytic hydrogenation qualities, a unique system might be at hand.

A new project will be started exploring a virtually ignored single observation in the literature involving an insertion reaction of a platinum complex into a benzene sp^2-sp^2 bond to give a metallacycloheptatriene. This transformation has clear potential in aromatic ring hydrogenolysis.

Hexamethyldisilane will be tested as a potential coal solubilization medium making use of the proven capacity of the trimethylsilyl group to function as a hydrogen analog.

Task 5: We will continue our relative reactivities studies, hoping to generate relative rates and define the inhibitory nature of other sulfur oxygen and nitrogen heterocycles under homogeneous catalytic hydrogenation conditions. Kinetics of hydrogen transfer will be investigated.

Task 6: A long-term goal of the project is to develop a theoretical model which can predict experimentally measured metal deposit profiles and desulfurization activities and which can be interpreted to find a pore structure that will

minimize catalyst deactivation from deposited metals. Our results to this point have shaped the framework of this model. Experiments in progress and planned for the near future are aimed at accurately determining model parameters. After completing the vanadyl porphyrin experiments in progress, the reaction apparatus will be modified for continuous operation and extensive titanyl porphyrin experiments begun. Continuous operation will yield more accurate rate constants and allow buildup of sufficient metal deposits to affect catalyst diffusity as measured by transient diffusity experiments.

TECHNICAL INFORMATION DEPARTMENT
LAWRENCE BERKELEY LABORATORY
UNIVERSITY OF CALIFORNIA
BERKELEY, CALIFORNIA 94720